

Photocatalytic degradation of anthracene using titanium dioxide-NPs doped with iron in the presence of UV radiation from the aqueous solution: by-products determination

Morteza Khodadadi Saloot^a, Seyed Mehdi Borghei^{b,*}, Reza Haji Seyed Mohammad Shirazi^c

^aDepartment of Environmental Engineering, Faculty of Natural Resources and Environment, Science and Research Branch, Islamic Azad University, Tehran, Iran, email: morteza.khodadadi.s@srbiau.ac.ir

^bDepartment of Chemical and Petroleum Engineering, Sharif University of Technology, Tehran, Iran, email: mborghei@sharif.edu

^cWater and Wastewater Engineering Division, Natural Resources and Environmental Engineering Department, Tehran Science and Research Branch, Islamic Azad University, Tehran, Iran, email: r-shirazi@srbiau.ac.ir

Received 21 August 2019; Accepted 13 December 2020

ABSTRACT

The aim of the present study was to evaluate the photocatalytic degradation of anthracene using Fe-doped TiO₂ nanoparticles in the presence of UV. The structure and morphology of Fe-doped TiO₂ nanoparticles were studied by X-ray diffraction, scanning electron microscopy, and energy-dispersive X-ray spectroscopy. The applied nanoparticles were synthesized by the sol-gel method. The effect of influential parameters on the degradation of anthracene, including pH, time, nanoparticles dosage, and the concentration of anthracene was studied. Using the UV/Fe-doped TiO₂ system, the optimum experimental values were obtained to be as follows: pH = 7, contact time = 60 min, anthracene concentration = 5 mg/L, and nanoparticle dosage = 100 mg/L. Based on the results, it could be concluded that the photocatalytic degradation of anthracene using the UV/Fe-doped TiO₂ provides suitable efficiency. In addition, it was found that the doped TiO₂ could be considered as a proper catalyst in photocatalytic degradation processes.

Keyword: Photocatalytic degradation; Fe-doped TiO₂-NPs; Anthracene; Aqueous solution; By-products

1. Introduction

Currently, the progress of the industries and the use and release of various types of chemicals have brought various adverse effects for all dimensions of the life cycle [1,2]. Polycyclic aromatic hydrocarbons (PAHs) are one of these pollutants which they are very toxic to the environment due to their resistance against degradation and can be associated with allergic, carcinogenic, and mutagenic properties [3,4]. These compounds are generally produced through anthropogenic activities; so that these activities are responsible to produce about 90% of these

compounds [4]. The anthracene is one of these compounds that is used in dyes, wood preservatives, and pesticides and is considered a highly toxic compound; so that it has classified as a carcinogen [5]. Hence, the degradation and removal of the PAH, especially anthracene, is essential.

Various methods have been proposed for removing these compounds in the aqueous environment. Physical and chemical methods such as flotation and the use of surfactants are costly and have a lot of limitations [5]. In general, conventional physical techniques such as flocculation, aeration, adsorption on activated carbon, and reverse osmosis may effectively eliminate the pollutants. However, these

* Corresponding author.

methods are not able to destruct the pollutants and only transfer the pollutants from water to another phase, which results in the formation of secondary environmental pollution that requires reprocessing and ultimately leads to increased costs. The photocatalyst is an advanced oxidation technology with a bright future and has been used to remove pollutants in the US, Europe, and Japan [6]. In recent years, the advanced oxidation processes have been identified as a flourishing method for advanced sewage treatment [7,8]. In these types of processes, potent oxidation agents (hydroxyl radicals) are produced, which can completely degrade the pollutants in the wastewater [9].

The photocatalytic and semiconductor process has been recognized as one of the most imperative techniques for wastewater treatment that it has found to be beneficial for removing the pollutants [10,11]. Among various semiconductor materials (oxides, sulfides, etc.), the brilliant properties of TiO_2 including the high photocatalytic activity, permanent chemical resistance to optical corrosion, economic acceptability, low-cost, and lack of toxicity has introduced it as the most relevant semiconductor in the context of the pollutant removal [12,13].

Although the high energy gap (3.2 eV) of TiO_2 has led to a decrease in the efficacy of its application, several methods have been developed to increase its photocatalytic activity such as increasing the surface-to-volume ratio, bonding TiO_2 to other semiconductor particles, spraying TiO_2 into the zeolite holes and doping the metal and non-metal ions TiO_2 [14]. The conductive metal ions can form a doped energy balance between conduction and capacities bonds of TiO_2 , which has been identified as an effective method to increase the activity of photocatalytic TiO_2 . In addition, the doped ions may act as electron traps or cavities and increase the catalytic activity of TiO_2 [15]. Studies have shown that the transition metal ions such as Fe^{3+} can be used to enhance the photocatalytic activity [16,17]. The Fe^{3+} ion metal can be easily placed between the TiO_2 networks due to its semi-filled electron arrangement and with ion radius close to ion Ti^{4+} radius and increases the photocatalyst activity in the visible light area. In addition, Fe^{3+} ions can also create a surface trap for electrons and cavities produced by radiation, which increases the photocatalytic activity by the reduction in the recombination of electrons and cavities [17]. Therefore, Fe^{3+} ion is considered an effective and significant doping agent. The purpose of this study was to determine the effect of photocatalytic degradation of anthracene using TiO_2 nanoparticles with iron in the presence of UV.

2. Materials and methods

2.1. Materials

All chemicals used in this study were of analytical grade. The chemicals including iron(III) nitrate nonahydrate ($\text{Fe}(\text{NO}_3)_3 \cdot 6\text{H}_2\text{O}$, CAS number: 7782-61-8), ethanol ($\text{C}_2\text{H}_5\text{OH}$, CAS number: 64-17-5), sodium hydroxide (NaOH , CAS number: 1310-73-2), and sulfuric acid (H_2SO_4 , CAS number: 7664-93-9) were provided from Merck (Germany). Other chemicals, that is, titanium dioxide (TiO_2 , CAS number: 13463-67-7) and titanium tetrachloride (TiCl_4 , CAS number: 7550-45-0), were provided from Sigma-Aldrich,

Shimadzu. Anthracene with the formula of $\text{C}_{14}\text{H}_{10}$ (the purity of >99%; CAS number: 120-12-7) was purchased from Merck & Co., (Germany). The pH of the solution was regulated using 0.1 M NaOH or 0.1 M H_2SO_4 . The required solutions were prepared using double distilled water.

2.2. Synthesis of Fe-TiO_2 nanoparticles

The sol-gel method was used to synthesize the Fe-TiO_2 nanoparticles. At first, 4.128 mL of TiCl_4 was dissolved in 70 mL of ethanol, and then 0.05 M of $\text{Fe}(\text{NO}_3)_3 \cdot 6\text{H}_2\text{O}$ and 2 mL water was added. In the next step, 17 mL propylene oxide was instilled at 50°C during the stirring of the prepared solution. After 5 min, a gel was formed and entered the process of aging for 48 h at room temperature; consequently, it was dried for 12 h at 80°C . The dried gel was calcined to obtain the anatase phase for 2 h at 350°C [10].

2.3. Photocatalytic experiments

This was a lab-scale study that was conducted to survey the ability of the photocatalytic degradation of anthracene using the Fe-TiO_2 . In this study, a reactor made of Pyrex was used for the photocatalytic degradation experiments. The diameter and height of this reactor were 180 and 150 mm and was used to hold 2 L of solution. The scheme of this photoreactor is presented in Fig. 1. A UVC lamp (125 W, Arad Co., France) was applied for irradiation experiments. The length and diameter of this lamp were 6.5 and 1 cm, respectively and it was placed on the center of one quartz tube which was sealed properly. The solution in the reactor was constantly mixing by a magnetic stirrer. The circulating of the cooling water by a pump was the used method to keep the temperature of this reactor at room temperature. The stock solution of anthracene (100 mg/L) was prepared, and other desired solutions were diluted from the stock solution. Ultraviolet light was used for anthracene photo-degradation using Fe-TiO_2 nanoparticle and the obtained. The effects of various parameters including, anthracene concentration (1–100 mg/L), the

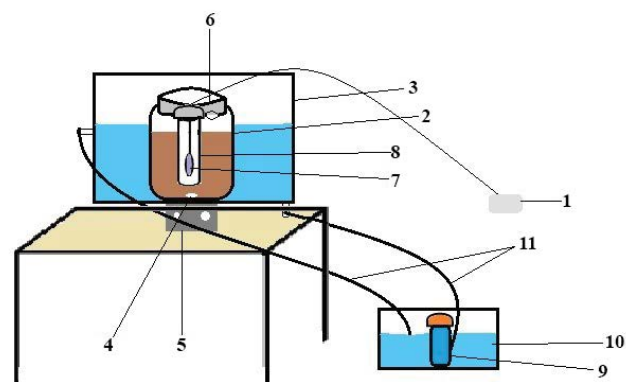


Fig. 1. Schematic of the reactor used in the process. (1) Trans of lamp 150 watt; (2) glass reactor; (3) cooling water; (4) magnet; (5) magnetic stirrer; (6) reactor doors; (7) UV lamp 150 watt medium pressure; (8) covering quartz; (9) pump; (10) water tank; (11) pipes for water.

dose of nanoparticles (50–300 mg/L), pH (3–11), and reaction time (10–180 min) were investigated in the study. The reactor was covered by aluminum foil to avoid the unwanted lights and their interference. The optimization method was applied to determine the size of the samples. The optimum amount of each parameter was obtained by varying one of the parameters while the other was kept constant.

2.4. Analytical methods

After conducting the related experiments, the samples were collected at predetermined time intervals and were centrifuged at 4,000 rpm for 30 min and then filtered through a 0.45 μm membrane filter and the concentration of anthracene was measured using high-performance liquid chromatography (HPLC). HPLC Agilent 1260 infinity (Agilent Technologies Co., Ltd., USA) equipped with a Shimadzu LC-20AB pump (140 mm \times 260 mm \times 420 mm, operating temperature range: 4°C–35°C, power requirements: 100 VAC, 150 VA, 50/60 Hz, maximum discharge pressure: 40 MPa, flow-rate setting range: 0.0001–10 mL/min, solvent delivery method: parallel-type double plunger, plunger capacity: 10 μL) was employed. A C18 column (250 mm \times 4.6 mm, with 5 μm particle size, pore size: 12 nm, surface area: 410 m^2/g , carbon loading: 20%, pore volume: 1.25 mL/g, pH range: 2–7.5, bonding type: monomeric), as the stationary phase, and a UV-Vis spectrophotometer (Shimadzu UV-1600, Japan, dimensions: 380 mm \times 550 mm \times 470 mm, power consumption: 160 VA, frequency: 50/60 Hz, wavelength range: 190–1,100 nm, wavelength accuracy: ± 0.5 nm, wavelength repeatability: ± 0.1 nm, photometric range: absorbance: -0.5 to $+3.999$ Abs, photometric accuracy (at 0.5 Abs): ± 0.002 Abs, photometric repeatability (at 0.5 Abs): ± 0.001 Abs) was used. The mobile phase was a mixture of water and methanol (40:60 v/v, HPLC grade, Merck, Germany) with a flow rate of 1 mL/min at 25°C. The mobile phase was a mixture of acetonitrile and deionized water (90:10 v/v) with a flow rate of 1 mL/min. The injection of 15 μL of anthracene solution into the column was done.

The efficiency of TiO_2 -NPs (NPs – nanoparticles) doped with iron in the presence of UV for degradation anthracene was calculated using Eq. (1):

$$\text{Degradation}(\%) = \left(\frac{C_0 - C_t}{C_0} \right) \times 100 \quad (1)$$

where C_0 and C_t correspond to the initial concentration of anthracene at the time 0 and the concentration of anthracene at time t , respectively.

The anthracene degradation intermediates analysis carried out using the liquid chromatography–mass spectrometry (LC/MS) (Shimadzu LCMS-2010A) system equipped with a C18 column (100 mm \times 2.1 mm) and an electron spray ionization source. All experiments were performed in triplicate.

The mineralogy of Fe-doped TiO_2 nanoparticles was also characterized by X-ray diffraction (XRD) techniques (Rigaku RINT 2200, Japan), and the surface morphology properties of Fe-doped TiO_2 nanoparticles were determined

using the scanning electron microscopy (SEM) technique (model KYKY-EM3200, Japan).

3. Results

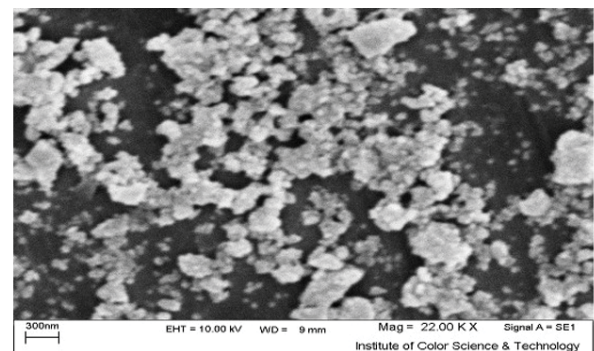
3.1. Characterization of nanoparticle studied

Fig. 2 is related to the SEM image and the distribution of TiO_2 nanoparticles diameter before doping with iron, respectively. The mean diameter of the nanoparticles was determined by the measurement software, and its results indicated the particles are in the nano-sized range. The mean diameter of the nanoparticles was observed to be 42.4 nm.

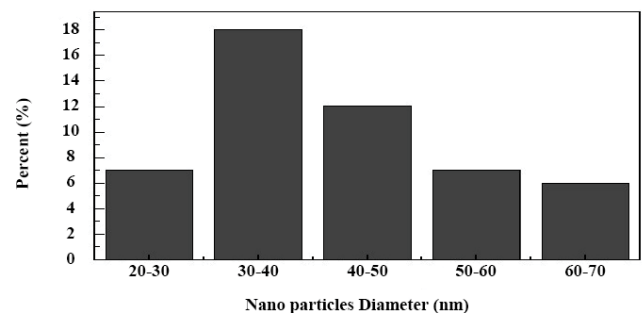
Fig. 3 demonstrates the SEM image and the distribution of the mean diameter of the Fe-doped TiO_2 nanoparticles, respectively. For these nanoparticles, the mean diameters were observed to be 37.89 nm. The comparison of the Fig. 3 related to TiO_2 and Fe- TiO_2 nanoparticles illustrates that the Fe- TiO_2 nanoparticles have a smaller structure while the TiO_2 particles have a bulky structure. Moreover, there is a smaller mean diameter for Fe-doped TiO_2 nanoparticles compared to TiO_2 nanoparticles.

Fig. 4 depicts the XRD pattern for Fe-doped TiO_2 nanoparticles. Considering the peaks in the diffraction pattern (at 25° maximum peaks), it is verified that the Fe-doped TiO_2 consists of an anatase structure.

The strong peaks observed at 27°, 36°, and 55° indicate that the TiO_2 is in the rutile phase. On the other hand, the peaks at 25° and 48° show that TiO_2 is in the anatase phase.

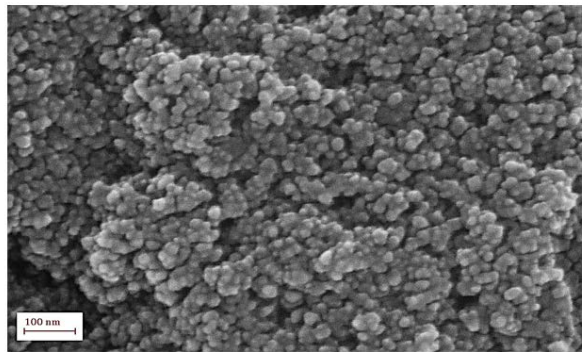


(a)

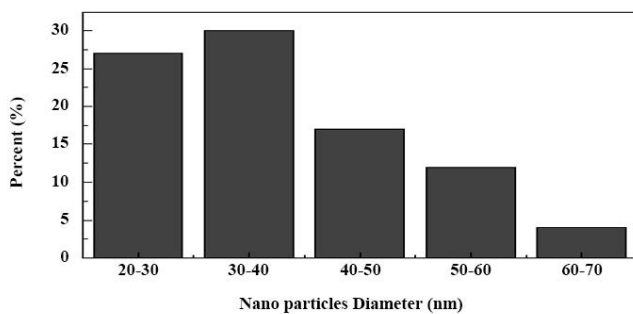


(b)

Fig. 2. (a) SEM image of the TiO_2 nanoparticles and (b) distribution of the TiO_2 nanoparticle diameter.



(a)



(b)

Fig. 3. (a) SEM image for the Fe-TiO₂ nanoparticles and (b) distribution of the Fe-TiO₂ nanoparticle diameter.

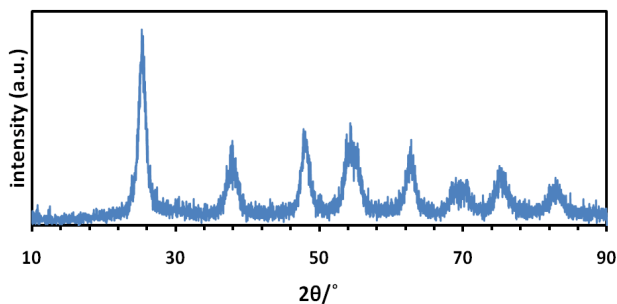


Fig. 4. X-ray diffraction pattern for Fe-doped TiO₂ nanoparticles.

Fig. 4 reveals that the maximum amount is related to the anatase phase. Titanium dioxide can be found in three crystalline forms, that is, the anatase, rutile, and brucite; however, the light catalytic activity can only be observed in anatase and rutile; it should be also mentioned that this characteristic is higher in the anatase phase compared to the rutile phase, hence the rutile phase is more appropriate.

3.2. Effect of pH on catalytic degradation in presence of UV radiation

The effect of pH on photocatalytic degradation of anthracene in the presence of UV radiation was studied at the different pH values (3, 5, 7, 9, and 11) by keeping constant the other parameters (time = 60 min,

anthracene concentration = 5 mg/L, and nanoparticle dosage = 100 mg/L); and the results were presented in Fig. 5. As observed, the highest anthracene degradation was observed at the pH values of 7 (97.22%), 5 (95.80%), and 9 (94.48%), respectively. Thus, the pH of 7 was selected as the optimum pH. Furthermore, Fig. 5 shows that the degradation efficiency decreases at pH values lower than 5 and higher than 11.

3.3. Effect of the reaction time on anthracene degradation in presence of UV

Fig. 6 represents the results of the effect of the reaction time on photocatalytic degradation of anthracene in presence of UV. For this purpose, the experiments were conducted by varying the reaction time (0, 30, 60, 90, and 120 min) at the constant values of pH = 7, anthracene concentration of 5 mg/L and nanoparticle dosage of 100 mg/L. The results indicate that the higher degradation efficiency is observed at the reaction times of 60 min (94.76%), 90 min (95.18%), and 120 min (95.64%). Therefore, the reaction time of 60 min was used as the optimum reaction time for further studies.

3.4. Effect of anthracene concentration on the removal of anthracene in the presence of UV radiation

Fig. 7 shows the results related to the effect of anthracene concentration on photocatalytic degradation efficiency. This study was conducted by keeping constant the other parameters, that is, pH of 7 and reaction time of 60 min and nanoparticles dosage of 100 mg/L and using different concentration of anthracene (5, 10, 25, 50, and 100 mg/L); the highest degradation percentage was achieved at the concentrations of 5 mg/L (97.89%), and 100 mg/L (91.5%), respectively. Thus, optimum anthracene concentration was elected as 5 mg/L.

3.5. Effect of TiO₂ nanoparticle dosage on the anthracene degradation efficiency in presence of UV radiation

The effect of this parameter was evaluated using the various nanoparticle dosage (50, 100, 150, 200, 250, and 300 mg/L) and by keeping constant the other parameters including pH of 7, anthracene concentration of 5 mg/L, and contact time of 60 min. The results are brought in Fig. 8. As can be seen, increasing the TiO₂ nanoparticle dosage increases anthracene degradation efficiency. The highest degradation efficiency was obtained at the dosages of 100 (%97.42%), 150 (%97.90), and 200 (%98.04) mg/L.

3.6. Effect of photolysis on anthracene degradation efficiency

Fig. 9 shows the effect of UV alone on the removal of anthracene at various contact times and pH values and a constant concentration of 100 mg/L of nanoparticles in aqueous solutions. Based on Fig. 9, it is observed that the effect of UV alone is low; so that the highest degradation percentage was obtained to be 26.09% at pH of 10 and contact time of 75 min. As the reaction time increases, the removal rate increases, but it remains constant after 60 min.

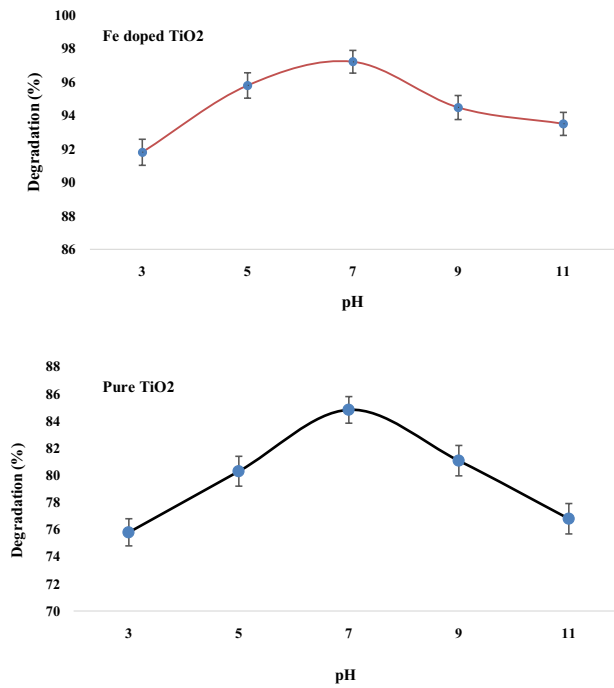


Fig. 5. Effect of pH on anthracene degradation in the presence of UV radiation.

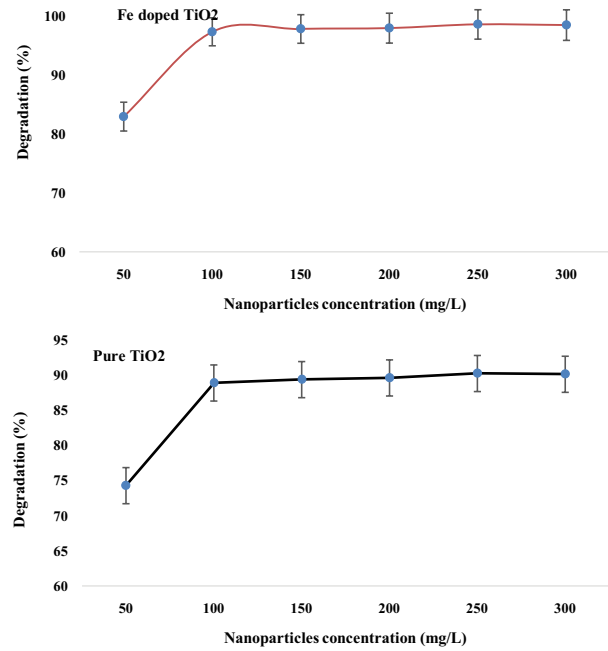


Fig. 8. Effect of concentration of nanoparticles on anthracene degradation in the presence of UV radiation.

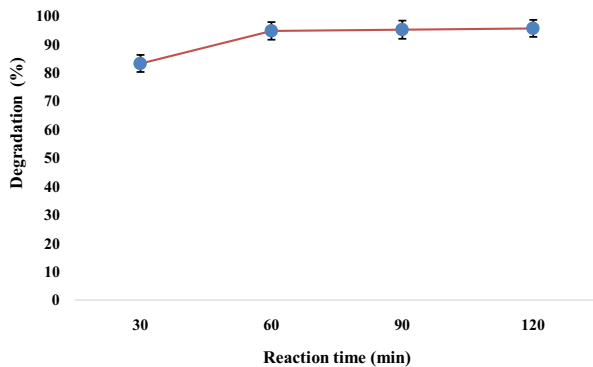


Fig. 6. Effect of contact time on anthracene degradation in the presence of UV radiation.

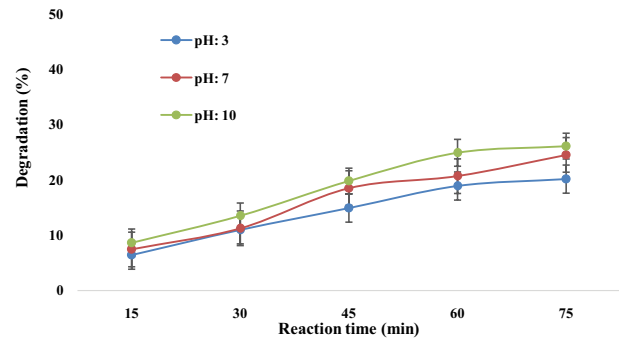


Fig. 9. Effect of UV alone on the anthracene degradation at different reaction times and pH values.

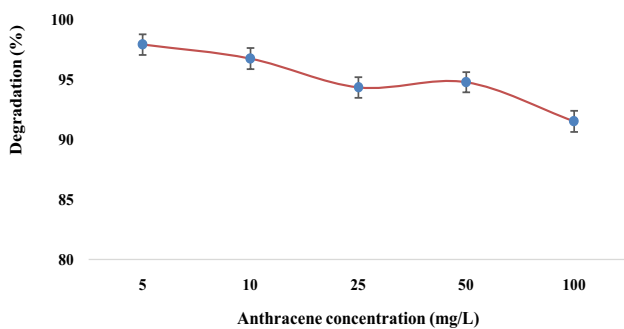


Fig. 7. Effect of anthracene concentration on anthracene degradation in the presence of UV radiation.

3.7. Comparison of the anthracene degradation efficiency using pure TiO₂ and Fe-doped TiO₂

Fig. 10 shows the results related to degradation of anthracene by pure TiO₂ and Fe doped TiO₂ in optimal condition. Considering Fig. 10, anthracene degradation efficiency by Fe-TiO₂ NPs was much higher than the pure TiO₂; so that the highest degradation efficiency by pure TiO₂ and Fe-TiO₂ NPs was achieved to be 55.32% and 98.13% after 60 min, respectively.

3.8. Identification of by-product in the photocatalytic degradation of anthracene

To detect the intermediates and products in the photocatalytic degradation of anthracene using TiO₂ NPs doped with iron in presence of UV radiation, a series of experiments were carried out at optimal condition (pH = 7, reaction

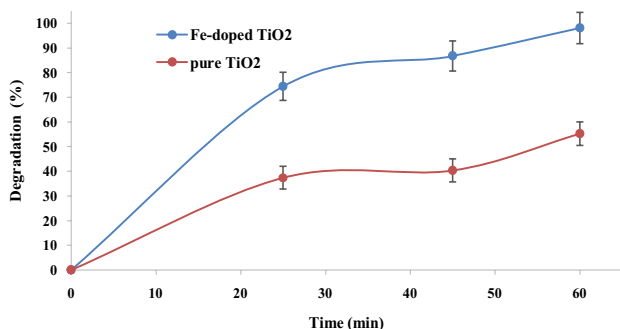


Fig. 10. Degradation of anthracene by the pure TiO₂ and Fe-doped TiO₂ in optimal condition (pH = 7; anthracene concentration = 5 mg/L; NPs concentration = 100 mg/L).

time = 60 min, anthracene concentration = 5 mg/L, NPs concentration = 100 mg/L) by LC-MS. Identified products and anthracene degradation pathways by LC-MS have been represented in Table 1; based on this, the main products were [anthrone], [9,10-dihydroxyanthracene], [9,10-anthraquinone], [phthalic acid], [4-formyl-benzoic acid ethyl ester], [benzoic acid], [protocatechuic acid], [benzaldehyde], and [pyrocatechol].

3.9. Comparison of degradation of anthracene using other methods

Table 2 reveals the comparison of the results obtained by the present study with the results of the other studies conducted for the removal and degradation of anthracene. Based on our observation, the removal and degradation of the anthracene have been assessed by a variety of methods, for example, modified zeolite (adsorption) process, biodegradation process, photocatalytic degradation process, immobilized peroxidase process, and alkaliphilic bacteria of *Bacillus badius* [3,18–22]. As provided in Table 2, the comparison between our studied system and other studies used for removal of anthracene was done based on various factors, that is, initial pH, reaction time, initial anthracene concentration, anthracene removal efficiency; this illuminated that our system used could reasonably provide greater anthracene degradation efficiency compared to the mentioned studies.

4. Discussion

The rate of chemical reactions depends on the pH of the environment and the pH, directly and indirectly, affects the oxidation of organic matter. In advanced oxidation processes, pH changes through the production of various radicals affect the rate of organic matter oxidation. Since the pH of the solution has a direct effect on the production of hydroxyl or sulfate radicals, and it affects the oxidation process efficiency, the pH is the first parameter that should be studied. pH is a vital variable in advanced oxidation processes and plays an imperative role in the acid-base equilibrium so that it affects the concentration of degraded or non-degraded material in the equation [23–25]. The most important cause of the effect of environmental pH

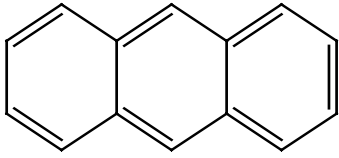
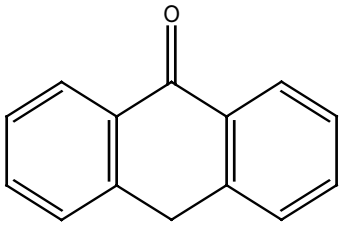
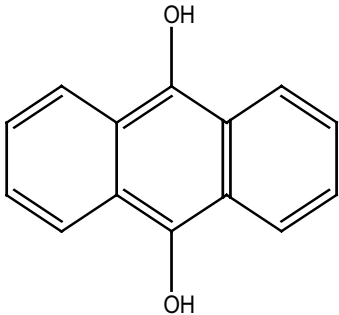
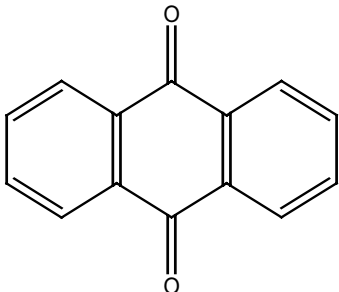
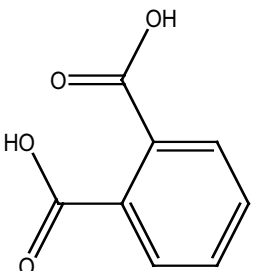
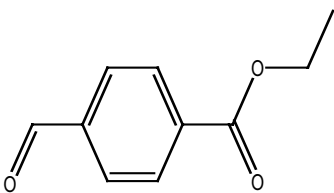
changes on the processes used in the degradation of organic compounds in advanced oxidation processes is the type and amount of radicals produced in the process which is caused by the presence of anions [26–28].

Investigating the effect of pH showed that the anthracene degradation rate is higher in neutral pH due to the presence of more OH⁻ ions in the alkaline environment. Moreover, the presence of catalysts can significantly reduce the oxygen molecules that existed in the solution to HO₂ radicals which eventually, become OH[•] radicals and these radicals can participate in increasing the anthracene degradation. The optimum pH for the degradation of anthracene under constant conditions in this study was observed to be 7 which the higher degradation efficiency was obtained at this pH and lower dosage of UV/Fe-doped TiO₂. Ghaly et al. [29] have observed that the chemical oxygen demand removal efficiency is 75% at the optimum TiO₂ dosage of 0.75, pH = 6.5 and at the contact time of 180 in the presence of sunlight. According to the results, the lowest percentage of anthracene removal is related to pH = 11, which can be due to the high concentration of hydroxyl in the alkaline environment because the excessive increase in hydroxyl concentration can be considered as a barrier to light penetration on TiO₂ surface. In addition, high pH causes the formation of carbonate ions, which is an effective scavenger for hydroxyl radicals and can reduce the rate of degradation [30].

The results of the study showed that the degradation efficiency was increased by increasing the reaction time from 10 to 90 and it reaches the equilibrium at a contact time of 60 min using the studied system in presence of UV. Based on these results, it was found that doping can reduce the time required to remove contaminants. Compared to other studies such as Kansal et al. [7], and Uğurlu and Karaoğlu [11], the removal of pollutants by the nano-photocatalytic method was low at the low reaction time, while the results of the present study indicated that the degradation of the anthracene was noteworthy at the contact time of 15 min and at the presence of UV using the Fe-doped TiO₂, which it can be due to Fe³⁺ metal ion [14] and increasing the photocatalytic activity by the presence of this ion. Ma et al. have reported that TiO₂ particles doped with platinum accelerate the electron-hole pair reaction, and therefore, it increases the concentrations of OH radicals on the surface of the catalyst and, as a result, increases photocatalytic degradation [31]. In addition, Fe³⁺ ions can create a surface trap for electrons in the TiO₂ network and the cavities created by the radiation; thus, by reducing the recombination of electrons and cavities, it increases the quantum yield and photocatalytic activity.

In this study, the highest removal efficiency was observed to be 98.53% by the studied system using 300 mg/L. Chang et al. [32] have observed the highest efficiency (close to 85%) using the nanoparticle dosage of 10 g/L; it illustrates that better results were obtained in the present study. Moreover, the results observed in the present work were much better than the results of Kumar et al. [33] and Kansal et al. [7]; in their study, the lower efficiency was achieved by the presence of a greater amount of nanoparticles. The better results in this study can be due to the use of the doped nanoparticle, which is in agreement with Ma et al. [31].

Table 1
Anthracene degradation pathways estimated by LC-MS data

Intermediate molecular structure	Scientific name	Molecular weight (g/mol)	Molecular formula
	Anthracene	178.23	C ₁₄ H ₁₀
	Anthrone	194.23	C ₁₄ H ₁₀ O
	9,10-Dihydroxyanthracene	210.23	C ₁₄ H ₁₀ O
	9,10-Anthraquinone	208.21	C ₁₄ H ₈ O ₂
	Phthalic acid	166.13	C ₈ H ₆ O ₄
	4-Formyl-benzoic acid ethyl ester	178.1846	C ₁₀ H ₁₀ O ₃

(Continued)

Table 1 Continued

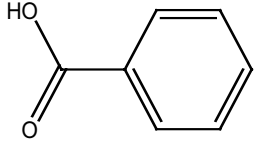
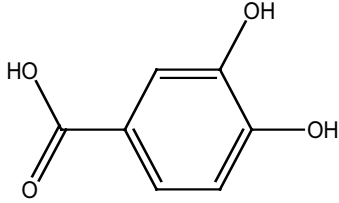
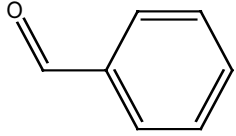
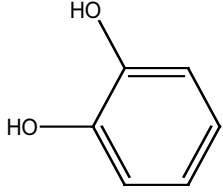
Intermediate molecular structure	Scientific name	Molecular weight (g/mol)	Molecular formula
	Benzoic acid	208	C ₇ H ₆ O ₂
	Protocatechuic acid	154.12	C ₇ H ₆ O ₄
	Benzaldehyde	106.12	C ₇ H ₆ O
	Pyrocatechol	110.1	C ₆ H ₆ O ₂

Table 2
Comparison of degradation of anthracene using other methods

Type of process	Parameters	Degradation (%)	References
Modified zeolite (adsorption) process	Conc. anthracene (1–20 mg/L); conc. modified zeolite (6–30 g/L); reaction time (20–120 min); pH (3–11)	99	[18]
Biodegradation process	Conc. anthracene (100–300 mg/L); contact time (24–72 h); pH (6.5–7.5)	51	[19]
Biodegradation process	Conc. anthracene (100–300 mg/L); contact time (1–7 d)	99	[20]
Photocatalytic degradation process	Conc. anthracene (23 mg/L); conc. catalyst (55.6 mg/L); reaction time (50–280 min); pH (7.2)	86.07	[21]
Immobilized peroxidase process	Conc. anthracene (5 mg/L); enzyme conc. (0.1–0.8 U/mL); reaction time (30–180 min); temperature (20°C–80°C); pH (2–10)	83.4	[3]
Photocatalytic degradation process	Conc. anthracene (5–25 mg/L); reaction time (30–180 min); UV light intensity (1–2.5 mW/cm ²); temperature (278–308°K); pH (6.8)	85	[22]
Alkaliphilic bacteria <i>Bacillus badius</i>	Conc. anthracene (50 mg/100 mL); salinity/NaCl (0.5%–3%); temperature (25°C–50°C); contact time (12–60 h); pH (6–11)	94.8	[23]
Photocatalytic degradation process	Conc. anthracene (1–100 mg/L); conc. NPs (50–300 mg/L); reaction time (10–180 min); pH (3–11)	98.13	Present study

The results of this study about the effect of the initial concentration of anthracene on photocatalytic degradation efficiency showed that increasing the initial concentration decreases the photocatalytic degradation efficiency.

Obviously, increasing the concentration of pollutants in the environment is led to more consumption of oxidizing

agents such as hydroxyl radicals. Reduction of removal efficiency by increasing the concentration of the pollutant can be interpreted by the fact that when a constant amount of hydroxyl radical, as oxidizing agents, at a constant time, is produced and entered the reaction reactor, the initial concentration of pollutants, as the consumer

of oxidizing agents, is increased. As a result, further presence of the oxidizing agent in the environment is not completely happened and is led to reducing the efficiency and producing the intermediate products [25,34,35].

Therefore, the degradation efficiency in the solution with a low initial concentration of pollutants will be greater than the solution with a higher initial pollutant concentration. In the present work, increasing the anthracene concentration decreases the degradation efficiency, which is consistent with the results of previous studies [36–39]. This phenomenon is described by the fact that increasing the pollutant concentration is led to lower photons absorption by the pollutant molecules, which resulted in less pollutant degradation and reducing the degradation efficiency.

The results also showed that the optimum dosage of nanoparticles in the removal of the anthracene is 100 mg/L. Therefore, according to the results of this study, in the presence of a very low nanoparticle dosage, there was a great degradation, which its main reason can be the doping of TiO₂ nanoparticles. Similar results were observed in the study conducted by Veisi et al. [40]; so that, the highest degradation of furfural by the photocatalytic process in presence of both UV and sunlight was obtained in lower nanoparticle dosage. In addition, it was observed that the efficiency of the TiO₂/SUN method compared to the TiO₂/UV was insignificant; its reason is the TiO₂ energy gap, which can only absorb the radiation at a wavelength of 278 and are not able to absorb a wide range of solar radiation. In the case of doped nanoparticles, due to the reduction of the energy gap, they are able to absorb a wider range of the sun wavelengths; thus, they have higher degradation efficiency. Also, the results of the study by Turek et al. [41] showed that the highest removal efficiency of PAHs was about 32%, which is lower than the present study.

About the degradability rate, results of the present study revealed that anthracene, after degradation, is converted into CO₂ and H₂O, which is consistent with results of similar studies conducted by Cui et al. [42], Ahmed et al. [43], Moody et al. [44], and Hassan et al. [45].

5. Conclusion

In the present work, the potential of the photocatalytic process in the degradation of anthracene using the Fe-doped TiO₂ nanoparticles in the presence of UV radiation was evaluated. The optimum values using the UV/Fe-doped TiO₂ system were obtained as follows: pH = 7, contact time = 60 min, anthracene concentration = 5 mg/L, and nanoparticle dosage = 100 mg/L. Also, since it could improve the biodegradability of anthracene containing solutions, it could be used as post-treatment in a bioreactor.

References

- [1] D. Balarak, J. Jaafari, G. Hassani, Y. Mahdavi, I. Tyagi, S. Agarwal, V.K. Gupta, The use of low-cost adsorbent (Canola residues) for the adsorption of methylene blue from aqueous solution: isotherm, kinetic and thermodynamic studies, *Colloid Interface Sci. Commun.*, 7 (2015) 16–19.
- [2] M. Pirsaeheb, A. Karami, K. Sharafi, A. Dargahi, A. Ejraei, Evaluating the performance of inorganic coagulants (polyaluminum chloride, ferrous sulfate, ferric chloride and aluminum sulfate) in removing the turbidity from aqueous solutions, *Int. J. Pharm. Technol.*, 8 (2016) 13168–13181.
- [3] Z. Karim, Q. Husain, Removal of anthracene from model wastewater by immobilized peroxidase from *Momordica charantia* in batch process as well as in a continuous spiral-bed reactor, *J. Mol. Catal. B: Enzym.*, 66 (2010) 302–310.
- [4] M. Afsharnia, M. Kianmehr, H. Biglari, A. Dargahi, A. Karimi, Disinfection of dairy wastewater effluent through solar photocatalysis processes, *Water Sci. Eng.*, 11 (2018) 214–219.
- [5] J.X. Fu, E.M. Suuberg, Thermochemical and vapor pressure behavior of anthracene and brominated anthracene mixtures, *Fluid Phase Equilib.*, 342 (2013) 60–70.
- [6] U. Akpan, B.H. Hameed, Parameters affecting the photocatalytic degradation of dyes using TiO₂-based photocatalysts: a review, *J. Hazard. Mater.*, 170 (2009) 520–529.
- [7] M. Samarghandi, A. Rahmani, G. Asgari, G. Ahmadidoost, A. Dargahi, Photocatalytic removal of cefazolin from aqueous solution by AC prepared from mango seed + ZnO under UV irradiation, *Global Nest J.*, 20 (2018) 399–407.
- [8] R.S. Yuan, R.B. Guan, P. Liu, J.T. Zheng, Photocatalytic treatment of wastewater from paper mill by TiO₂ loaded on activated carbon fibers, *Colloids Surf.*, A, 293 (2007) 80–86.
- [9] K. Hasani, A. Peyghami, A. Moharrami, M. Vosoughi, A. Dargahi, The efficacy of sono-electro-Fenton process for removal of Cefixime antibiotic from aqueous solutions by response surface methodology (RSM) and evaluation of toxicity of effluent by microorganisms, *Arabian J. Chem.*, 13 (2020) 6122–6139.
- [10] S.K. Kansal, M. Singh, D. Sud, Studies on photodegradation of two commercial dyes in aqueous phase using different photocatalysts, *J. Hazard. Mater.*, 141 (2007) 581–590.
- [11] M. Uğurlu, M.H. Karaoğlu, Removal of AOX, total nitrogen and chlorinated lignin from bleached Kraft mill effluents by UV oxidation in the presence of hydrogen peroxide utilizing TiO₂ as photocatalyst, *Environ. Sci. Pollut. Res.*, 16 (2009) 265–273.
- [12] N. Guettaï, H.A. Amar, Photocatalytic oxidation of methyl orange in presence of titanium dioxide in aqueous suspension. Part I: parametric study, *Desalination*, 185 (2005) 427–437.
- [13] N. Guettaï, H.A. Amar, Photocatalytic oxidation of methyl orange in presence of titanium dioxide in aqueous suspension. Part II: kinetics study, *Desalination*, 185 (2005) 439–448.
- [14] Z. Mesgari, M. Gharagozlou, A. Khosravi, K. Gharanjig, Spectrophotometric studies of visible light induced photocatalytic degradation of methyl orange using phthalocyanine-modified Fe-doped TiO₂ nanocrystals, *Spectrochim. Acta, Part A*, 92 (2012) 148–153.
- [15] G.G. Liu, X.Z. Zhang, Y.J. Xu, X.S. Niu, L.Q. Zheng, X.J. Ding, The preparation of Zn²⁺-doped TiO₂ nanoparticles by sol-gel and solid phase reaction methods respectively and their photocatalytic activities, *Chemosphere*, 59 (2005) 1367–1371.
- [16] M.H. Zhou, J.G. Yu, B. Cheng, Effects of Fe-doping on the photocatalytic activity of mesoporous TiO₂ powders prepared by an ultrasonic method, *J. Hazard. Mater.*, 137 (2006) 1838–1847.
- [17] L. Sun, J. Li, C.L. Wang, S.F. Li, H.B. Chen, C.J. Lin, An electrochemical strategy of doping Fe³⁺ into TiO₂ nanotube array films for enhancement in photocatalytic activity, *Sol. Energy Mater. Sol. Cells*, 93 (2009) 1875–1880.
- [18] N. Rafieal-Hosseini, A. Ebrahimi, S.M. Borghei, Evaluation of the removal efficiency of anthracene from aqueous solution using natural zeolite compared to modified zeolite, *Health Syst. Res.*, 13 (2017) 180–186.
- [19] Z. Yousefi, R. Safari, S. Sarvi, R.A. Mohammadpour Tahmtan, E. Rostamali, Anthracene biodegradation by bacteria isolated from Tajan River Estuary, *J. Mazandaran Univ. Med. Sci.*, 24 (2014) 111–122.
- [20] M. Habibi, M.M.J. Mehdipour, M.A. Zanjanchi, Biodegradation of anthracene by *Bacillus* sp. in wastewater contaminated with polycyclic aromatic hydrocarbons, *Biol. J. Microorganism*, 5 (2016) 106–116.
- [21] M.A. Sliem, A.Y. Salim, G.G. Mohamed, Photocatalytic degradation of anthracene in aqueous dispersion of metal oxides nanoparticles: effect of different parameters, *J. Photochem. Photobiol. A*, 371 (2019) 327–335.

- [22] F.F. Karam, F.H. Hussein, S.J. Baqir, A.F. Halbus, R. Dillert, D. Bahnemann, Photocatalytic degradation of anthracene in closed system reactor, *Int. J. Photoenergy*, 2014 (2014) 503825, <https://doi.org/10.1155/2014/503825>.
- [23] A. Seid-Mohammadi, G. Asgarai, Z. Ghorbanian, A. Dargahi, The removal of cephalixin antibiotic in aqueous solutions by ultrasonic waves/hydrogen peroxide/nickel oxide nanoparticles (US/H₂O₂/NiO) hybrid process, *Sep. Sci. Technol.*, 55 (2020) 1558–1568.
- [24] M.R. Samarghandi, D. Nematollahi, G. Asgari, R. Shokoohi, A. Ansari, A. Dargahi, Electrochemical process for 2,4-D herbicide removal from aqueous solutions using stainless steel 316 and graphite anodes: optimization using response surface methodology, *Sep. Sci. Technol.*, 54 (2019) 478–493.
- [25] A. Zarei, H. Biglari, M. Mobini, A. Dargahi, G. Ebrahimzadeh, M.R. Narooie, E.A. Mehrizi, A.R. Yari, M.J. Mohammadi, M.M. Baneshi, R. Khosravi, M. Poursadeghiyan, Disinfecting poultry slaughterhouse wastewater using copper electrodes in the electrocoagulation process, *Pol. J. Environ. Stud.*, 27 (2018) 1907–1912.
- [26] A. Dargahi, D. Nematollahi, G. Asgari, R. Shokoohi, A. Ansari, M.R. Samarghandi, Electrodegradation of 2,4-dichlorophenoxyacetic acid herbicide from aqueous solution using three-dimensional electrode reactor with G/β-PbO₂ anode: Taguchi optimization and degradation mechanism determination, *RSC Adv.*, 8 (2018) 39256–39268.
- [27] A. Zarei, H. Biglari, M. Mobini, G. Ebrahimzadeh, A.R. Yari, M.R. Narooie, E.A. Mehrizi, A. Dargahi, M.M. Baneshi, M.J. Mohammadi, S. Mazloomi, Enhancing electrocoagulation process efficiency using *Astraglus gossypinus* tragacanth in turbidity removal from brackish water samples, *Pol. J. Environ. Stud.*, 27 (2018) 1858–1851.
- [28] A. Dargahi, A. Ansari, D. Nematollahi, G. Asgari, R. Shokoohi, M.R. Samarghandi, Parameter optimization and degradation mechanism for electrocatalytic degradation of 2,4-dichlorophenoxyacetic acid (2,4-D) herbicide by lead dioxide electrodes, *RSC Adv.*, 9 (2019) 5064–5075.
- [29] M.Y. Ghaly, T.S. Jamil, I.E. El-Seesy, E.R. Souaya, R.A. Nasr, Treatment of highly polluted paper mill wastewater by solar photocatalytic oxidation with synthesized nano TiO₂, *Chem. Eng. J.*, 168 (2011) 446–454.
- [30] M.R. Samarghandi, A. Dargahi, A. Shabanloo, H.Z. Nasab, Y. Vaziri, A. Ansari, Electrochemical degradation of methylene blue dye using a graphite doped PbO₂ anode: optimization of operational parameters, degradation pathway and improving the biodegradability of textile wastewater, *Arabian J. Chem.*, 13 (2020) 6847–6864.
- [31] Y.-S. Ma, C.-N. Chang, Y.-P. Chiang, H.-F. Sung, A.C. Chao, Photocatalytic degradation of lignin using Pt/TiO₂ as the catalyst, *Chemosphere*, 71 (2008) 998–1004.
- [32] C.-N. Chang, Y.-S. Ma, G.-C. Fang, A.C. Chao, M.-C. Tsai, H.-F. Sung, Decolorizing of lignin wastewater using the photochemical UV/TiO₂ process, *Chemosphere*, 56 (2004) 1011–1017.
- [33] P. Kumar, S. Kumar, N.K. Bhardwaj, A.K. Choudhary, Advanced Oxidation of Pulp and Paper Industry Effluent, Proceedings of the 2011 International Conference on Environmental and Agriculture Engineering (ICEAE 2011), IACSIT Press, Singapore, 2011, pp. 29–31.
- [34] A. Dargahi, M. Pirsahab, S. Hazrati, M. Fazlzadehdavil, R. Khamutian, T. Amirian, Evaluating efficiency of H₂O₂ on removal of organic matter from drinking water, *Desal. Water Treat.*, 54 (2015) 1589–1593.
- [35] A. Almasi, A. Dargahi, M. Mohammadi, A. Azizi, A. Karami, F. Baniamerian, Z. Saeidimoghadam, Application of response surface methodology on cefixime removal from aqueous solution by ultrasonic/photooxidation, *Int. J. Pharm. Technol.*, 8 (2016) 16728–16736.
- [36] S.M. Borghai, S.N. Hosseini, Comparison of furfural degradation by different photooxidation methods, *Chem. Eng. J.*, 139 (2008) 482–488.
- [37] S. Singh, V.C. Srivastava, I.D. Mall, Fixed-bed study for adsorptive removal of furfural by activated carbon, *Colloids Surf., A*, 332 (2009) 50–56.
- [38] A.K. Sahu, V.C. Srivastava, I.D. Mall, D.H. Lataye, Adsorption of furfural from aqueous solution onto activated carbon: kinetic, equilibrium and thermodynamic study, *Sep. Sci. Technol.*, 43 (2008) 1239–1259.
- [39] M.M. Selseleh, H. Keshavarz, M. Mohebbi, S. Shojaee, M.H. Modarressi, M.R. Eshragian, M.M. Selseleh, Production and evaluation of *Toxoplasma gondii* recombinant surface antigen 1 (SAG1) for serodiagnosis of acute and chronic *Toxoplasma* infection in human sera, *Iran J. Parasitol.*, 7 (2012) 1–9.
- [40] F. Veisi, M.A. Zazouli, M.A. Ebrahimzadeh, J.Y. Charati, A.S. Dezfoli, Photocatalytic degradation of furfural in aqueous solution by N-doped titanium dioxide nanoparticles, *Environ. Sci. Pollut. Res.*, 23 (2016) 21846–21860.
- [41] A. Turek, M. Włodarczyk-Makuła, W.M. Bajdur, Effect of catalytic oxidation for removal of PAHs from aqueous solution, *Desal. Water Treat.*, 57 (2016) 1286–1296.
- [42] C.Z. Cui, L. Ma, J. Shi, K.F. Lin, Q.S. Luo, Y.D. Liu, Metabolic pathway for degradation of anthracene by halophilic *Marteella* sp. AD-3, *Int. Biodeterior. Biodegrad.*, 89 (2014) 67–73.
- [43] A.T. Ahmed, M.A. Othman, V.D. Sarwade, G. Kachru, Degradation of anthracene by alkaliphilic bacteria *Bacillus badius*, *Environ. Pollut.*, 1 (2012) 97–104.
- [44] J.D. Moody, J.P. Freeman, D.R. Doerge, C.E. Cerniglia, Degradation of phenanthrene and anthracene by cell suspensions of *Mycobacterium* sp. strain PYR-1, *Appl. Environ. Microbiol.*, 67 (2001) 1476–1483.
- [45] S.S.M. Hassan, W.I.M. El Azab, H.R. Ali, M.S.M. Mansour, Green synthesis and characterization of ZnO nanoparticles for photocatalytic degradation of anthracene, *Adv. Nat. Sci.: Nanosci. Nanotechnol.*, 6 (2015) 045012.